

Research Article**CFD performance analysis for Darrieus Hydrokinetic Turbine****Humberto Rolong Ortiz¹, Carlos Acevedo Penaloza² and Guillermo Valencia Ochoa^{3,*}**¹Laboratório de energia solar – LABSOL, Escola de Engenharia da Universidade Federal do Rio Grande do Sul, Porto Alegre – RS, 15049, Brasil²Facultad de Ingeniería, Universidad Francisco de Paula Santander, Avenida Gran Colombia No. 12E-96, Cúcuta, Norte de Santander, Cúcuta, 01012, Colombia³Departamento de Ingeniería Mecánica, Universidad del Atlántico, Carrera 30 Número 8-49, Puerto Colombia, Barranquilla 080007, Colombia

Received 28 August 2018; Accepted 10 April 2019

Abstract

This work proposes the analysis of the behavior of a Darrieus type hydrokinetic turbine, starting from the mathematical model that allows to delimit the operation system, linking all the variables present in the phenomenon, specifically the fluid properties such as density, velocity, viscosity and Reynolds number. Also considered are the geometric data of the profiles, the rope length, cross-sectional area, angle of attack of the impeller, type of profile used and speed of rotation. The initial domain data, the flow area and the boundary conditions are selected to solve the model and thus obtain the data of the individual behavior of the selected profiles. For this, the lift and drag curves are obtained over a wide range of angles of attack. After characterizing the profile, the behavior of the impeller is simulated, calculating its power coefficient and consequently its performance.

Keywords: Angle of attack, drag curve, lift curve, Darrieus, simulation, hydrokinetic turbine.

1. Introduction

Currently, the high environmental costs of generating energy from fossil fuels have produced the highest amount of greenhouse gas emissions to the atmosphere in the last 20 years. This was the key piece that drove the development of alternative sources of energy with low environmental impact.

According to data from the Superintendence of Public Services by 2012, it is estimated that the areas not interconnected to the National Electricity Network represent 66% of the national territory (ZNI), which are made up of geographically isolated populations, located in Orinoco, the Amazon, the Pacific Coastal Platform, San Andrés, Providencia and Santa Catalina. Other data show that the areas of difficult connection to the National Interconnected System are inhabited by around 1,800,000 people, located in 1,199 localities. Electricity service coverage is 34% in these areas and service is 96% dependent on fossil-fuel thermal power plants [1].

Considering the current situation in Colombia, when the end of the armed conflict is being signed, which has largely had to do with the historical abandonment of rural areas, it is necessary and essential to look for alternatives that will allow the modernization of the countryside. The figures are very telling, the country has a huge demand that needs to be met in the medium term to reach acceptable levels of competitiveness to meet the challenges of post-conflict and

the already signed Free Trade Agreements.

The most viable option to meet this energy demand comes from renewable sources, as it meets the objective of being environmentally friendly and replaces the need of rural populations for electricity. Studying the theoretical allows us to understand the operation and the aerodynamic or hydrodynamic characteristics of machines that operate based on clean energies, such as hydrokinetic energy. In this work we propose to analyze the behavior of a Darrieus type hydrokinetic turbine, widely studied in the engineering field. Fundamental study variables of the working fluid are categorized as density, speed, turbulence, viscosity and Reynolds number.

It should be noted that in the market there are rotor models, whose technical information has been restricted by the manufacturers, so there is a need to obtain the mathematical model that allows the study system of a specific turbine to be delimited with its own geometric and profile data such as the length of the rope, cross-sectional area, angle of attack; of the impeller such as: the diameter, type of profile used, rotation speed.

Once the model is solved based on the initial operation data, flow area domain and contour conditions, the lift and drag curves for a wide range of angles of attack are obtained by deducing the individual behavior of the profiles used. Finally, the behavior of the impeller is simulated by calculating its power coefficient. The computational fluid tool helps to have a more affordable, dynamic and precise handling of the equipment's operation, to such an extent that its performance can be evaluated, validating with certainty how its studies will behave in the real world.

*E-mail address: ov.guillermovalencia@gmail.com

ISSN: 1791-2377 © 2019 Eastern Macedonia and Thrace Institute of Technology. All rights reserved.

doi:10.25103/jestr.122.06

2. Methodology

The type of turbine used in this work was selected based on its multidirectional flow function, which is why the most suitable model was the Darrieus type H [2], its shown in Figure 1. These turbines base their movement on the carrying force caused by the fluid, and their blades are shaped like wing profiles. These turbines can reach high efficiencies and speeds, approaching the Betz limit [3].

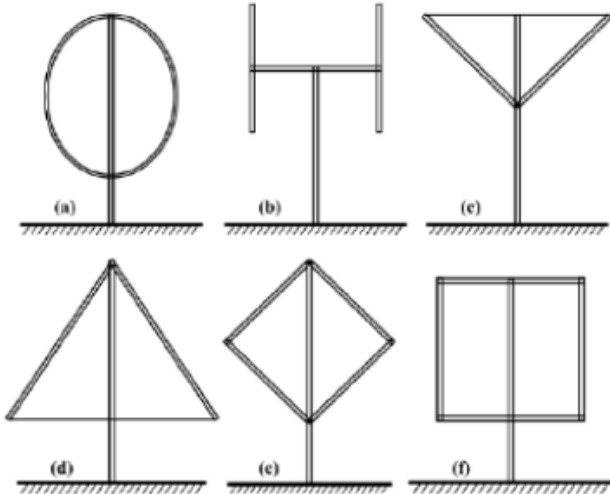


Fig 1. Configurations of different Darrieus turbines
 Fig 1. Configurations of different Darrieus turbines

Multiple designs were tested between 1979 and 1980, but due to fatigue failures they were unsuccessful. Today, due to new materials that provide better mechanical properties, models have been built that can reliably withstand fatigue loads. [4]

2.1. Double mathematical modeling of multiple current tubes

In order to study Darrieus turbines, several theories have been developed to predict their behaviour. The model used in this study is the model known as the Double Multiple Streamtube developed by Ion Paraschivoiu [5]. It was decided to use this method because of its simplicity and low computational cost. The model was created to study wind turbines, however the flow of water having a Mach number less than 0.3 is considered as an incompressible fluid changing from one to the other the density and viscosity.

The model is based on the principle of conservation of momentum in a quasi-stable flow and is matched with the forces on the rotor blades that change the momentum of flow within the turbine. There are three categories of analytical models: simple current tube; which assumes that the entire turbine is enclosed in a single current tube, the multi-tube current tube; which divides the rotor into several adjacent tubes and the multi-tube double-tube current tube that resembles the multi-tube tube but divides the rotor into two aerodynamically independent actuating discs located in series. The main difference between all these methods is the way the induced velocity is calculated.

The calculation of the induced speed through the rotor is based on the principle of the two tandem actuating discs at each rotor level as shown in Figure 2. In this, the velocity distribution over the turbine is shown by dividing it into 4 representative speeds: U_∞ ; which is the free flow speed, U_i ; which is the local vane speed at the top, U_e ; which is the equilibrium speed at the centre of the turbine, U_i' ; which is

the local vane speed at the bottom of the turbine and U_w which is the free flow speed at the outlet.

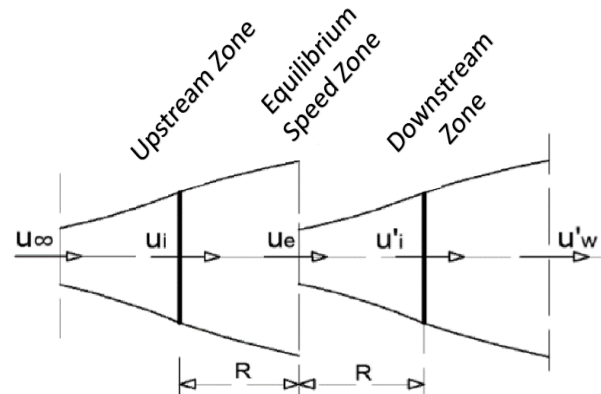


Fig 2. Velocity distribution.

For the calculation of the velocities in the upper part of the turbine or first actuating disc, a term called induction factor $u < 1$ is taken into account, which is a flow interference factor that relates the upstream local induced velocity as shown in Figure 3. This is calculated by means of

$$U_i = U_\infty * u. \quad (1)$$

The balancing speed is given by

$$U_e = (2u - 1) * U_i \quad (2)$$

The downstream blade speed is $U_i' = U_e * u'$ therefore $u' = U_i' / U_e$, in which $u' < u$. Under these conditions the value of u' and u is calculated from a double iteration in each current tube for each half of the turbine, as shown in Figure 3.

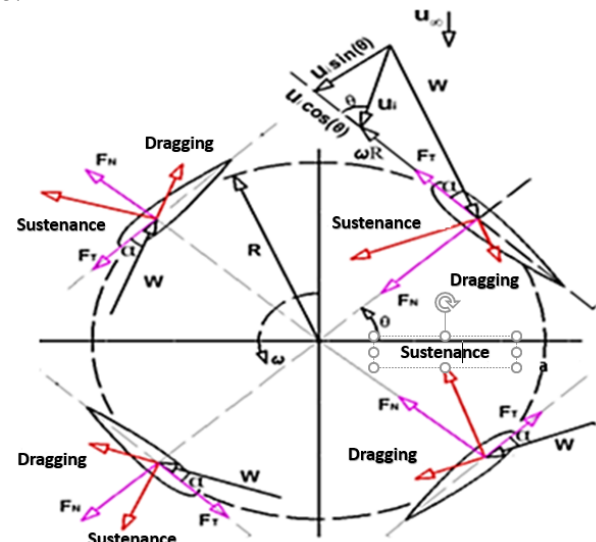


Fig 3. DMST Scheme

The first half of the impeller is comprised of $-90 \leq \theta \leq 90$. The relative velocity upstream is as follows:

$$W_U = \sqrt{U_i^2((X - \sin\theta) + \cos^2\theta)} \quad (3)$$

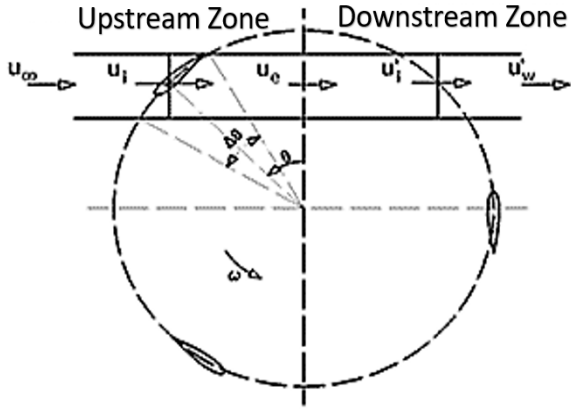


Fig 4. Velocity distribution of angles and forces at the impeller

From Figure four you can derive the equation that defines the angle of attack [6] as:

$$\alpha = \sin^{-1} \left[\frac{\cos \theta}{\sqrt{(X - \sin \theta)^2 + \cos^2 \theta}} \right] \quad (4)$$

Where $X = \omega * R / U_i$ is the TSR for the upstream part of the rotor. Using the theory of momentum conservation for each current tube in terms of the interference factor u , where $u = U_x / U_i$

$$f_{up} u = \pi(1 - u) \quad (5)$$

Where f_{up} is the function that characterizes the upstream half of the rotor, in the rotary blade element in that area. Taking into account these considerations for upstream this function is given by:

$$f_{up} = \frac{Nc}{8\pi R} \int_{-\pi/2}^{\pi/2} \left(C_N \frac{\cos \theta}{|\cos \theta|} - C_T \frac{\sin \theta}{|\cos \theta|} \right) \left(\frac{W}{U_i} \right)^2 d\theta \quad (6)$$

C_N and C_T are the normal and tangential forces affecting the blade, and are defined by:

$$C_N = C_L \cos \alpha + C_D \sin \alpha \quad (7)$$

$$C_T = C_L \sin \alpha - C_D \cos \alpha \quad (8)$$

C_D and C_L are the drag and carry coefficients respectively, which are calculated by the Montgomerie extrapolation method. To obtain these coefficients use the local Reynolds

$$Re_b = \frac{Wu * c}{U_\infty} \quad (9)$$

Therefore, for a given geometry, defined angular velocity ω , a distribution of current tubes and a value of $u=1$ assumed; a first value of X is calculated, the relative velocity Wu and the angle of attack α are found. From these values the local Reynolds Re_b is calculated and extrapolated between the C_N and C_T data by the Montgomerie method [7]. From these, the f_{up} function derived from the rotating blade element theory in that area is calculated and compared with the f_{up} function in Eq. 5. Both equations are equalised and the value of u is cleared, if both values are close enough with a difference of 0.003 the value is considered to have converged and the next current tube is passed where the same procedure is performed iteratively until the first half of the impeller or upstream half is completed.

The second half is comprised of $90 \leq \theta \leq 270$. The relative velocity in the downstream blade is calculated by the following expression:

$$W_D = \sqrt{U_i'^2 ((X' - \sin \theta) + \cos^2 \theta)} \quad (10)$$

Where $X' = \omega * R / U_i'$ is the local TSR at the bottom of the rotor blade. In addition $U_i'^2$ is the function of the induction factors u and u' and of the equilibrium velocity U_e .

The local angle of attack is defined as:

$$\alpha' = \sin^{-1} \left[\frac{\cos \theta}{\sqrt{(X' - \sin \theta)^2 + \cos^2 \theta}} \right] \quad (11)$$

Following the same procedure as in the first part of the rotor, and using the theory of momentum conservation for each current tube in terms of the interference factor u' , where $u' = U_d / U_d$ is deduced:

$$f_{down} u' = \pi(1 - u') \quad (12)$$

Where f_{down} is the function that characterizes the downstream half of the rotor, in the rotary blade element in that area. Taking into account these considerations for downstream this function is given by:

$$f_{down} = \frac{Nc}{8\pi R} \int_{-\pi/2}^{\pi/2} \left(C_N' \frac{\cos \theta}{|\cos \theta|} - C_T' \frac{\sin \theta}{|\cos \theta|} \right) \left(\frac{W_D}{U_i'} \right)^2 d\theta \quad (13)$$

The procedure described above is followed with the difference that the iteration begins with $u' = u$ and ends when the proposed convergence criterion of 0.003 is reached, as in the first half. If the iteration does not converge, it is taken as the induction factor value in the first half for the analyzed current tube. After obtaining valid data the coefficients of normal and tangential forces C_N and C_T respectively, the instantaneous T_i torque is calculated:

$$T_i = \frac{1}{2} \rho c R l C_T W^2 \quad (14)$$

Where ρ is the density of the fluid, c is the length of the cord, l is the height of the blade and W is the relative speed of the blade in that current tube. Calculate the torque in each current tube in both halves of the turbine, then proceed to calculate the average torque in the first half by adding up all the instantaneous torques using Eq. 15.

$$T_{prom} = N \sum_{i=1}^{N_{tc}} \frac{\frac{1}{2} \rho c R l C_T W^2}{N_{tc}} \quad (15)$$

Where N is the number of blades and N_{tc} is the number of current tubes. The torque coefficient CT can be defined as:

$$CT = \frac{T_{prom}}{\frac{1}{2} \rho S_b U_\infty^2} \quad (16)$$

Where S is the scanning area of the pallet defined as $S_b = 2 * l * R$. Having calculated the torque coefficient you can calculate the power coefficient CP for each half of the turbine $CP = C_T * \lambda$ and to obtain the overall power coefficient CP_g of the turbine simply add both power coefficients together $CP_g = CP_1 + CP_2$.

2.2. Turbine Simulation

To validate the results obtained in the mathematical model, the simulation is carried out on the Fluent platform of the company Ansys Inc.

2.2.1 Pre-processing

It is the first step of the simulation, in it, the domain to be studied is formed, in this case, the sliding mesh technique was used. Figure 5 shows how the rotor domain or mobile domain and the surrounding fluid or static domain are delimited.

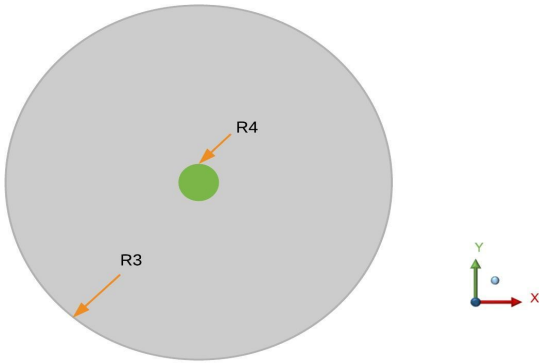


Fig 5. R4 rotary domain and R3 static domain

The impeller geometry was developed in ICEM, a Fluent platform specialized in the generation of meshes for studies related to fluid mechanics.

As shown in Figure 6, it is decided to divide the domain into 3 parts because the blades are distributed periodically every 120°, this allows to reduce mesh time and keeps the symmetry in all the blades, having the same density of elements in the wall for each one.

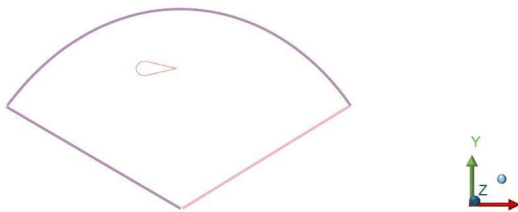


Fig 6. Meshed domain.

For the creation of the hydrodynamic profile, the coordinates of the page specialized in profiles "aifooltools.com" were obtained from which the file ".txt" is extracted, which is imported into ICEM. This profile was given the string size according to the data taken from the mathematical modeling. The geometries were developed according to the parameters in Table 1.

Table 1. Design parameters

Property	Unit	Value
Turbine radius	[m]	3
Degree of solidity	σ [-]	0.25
Breadth	b[m]	1
Area	A[m ²]	0.75
N° Vanes	N[-]	3
String	C[m]	0.25
Profile	[-]	DU06-W200

ICEM creates blocks that are composed of axes and vertices, these in turn are associated with the geometry, the creation of the blocks allows giving special characteristics to the mesh in sections where it is required to mesh more precisely, for example in the vane, as shown in Figure 7.

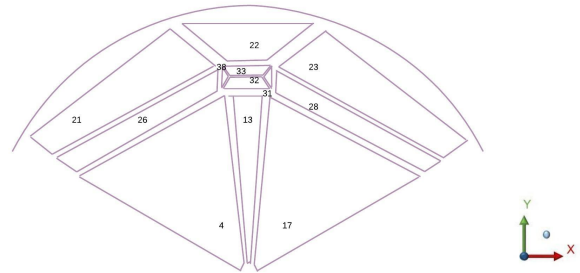


Fig 7. Mesh blocks

Blocks are divisions of the area that allow each to mesh independently, which is the most important characteristic of unstructured meshes.

The axes are then divided into the number of required elements, differentiating the blade, where special treatment must be given using an O-type mesh also known as O-grid, which means that the mesh lines follow an ordered pattern, enclosing the geometry following a concentric pattern. An O-grid was created around each blade, with a refinement near the blade wall and around the shaft wall, in order to homogeneously and neatly accommodate the nodes to the geometry to facilitate the calculation of the fluid behavior.

2.2.2 Wall refinement

Since large pressure and velocity gradients are at the boundary layer, special care must be taken to generate a sufficiently refined mesh in the wall, which allows these phenomena to be captured in detail.

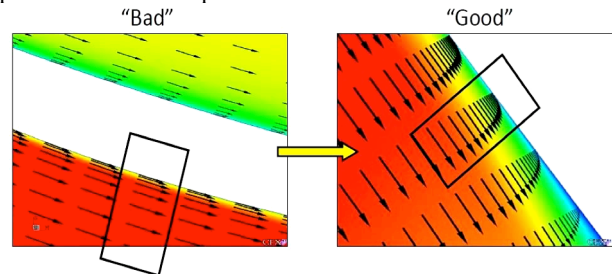


Fig 8. Flow physics

As can be seen in Figure 8, on the left side, the velocity gradient at the boundary layer does not show correctly the variation in the flow development on the surface, thus generating erroneous results [8]. This refinement is made on the basis of a dimensionless parameter known as y^+ , which allows the distance to the first cell of the wall defined by equation (17) to be calculated.

$$y^+ = \frac{\rho \cdot u_t \cdot y}{\mu} \quad (17)$$

Where y is the normal distance from the wall, μ_t is the friction velocity and is defined by the following expression:

$$\mu_t = \sqrt{\frac{\tau_w}{\rho}} \quad (18)$$

Where τ_w is the shear stress on the wall:

$$\tau_w = C_f * \frac{1}{2} * \rho * (V_0)^2 \quad (19)$$

And C_f is

$$C_f = [2 * \log_{10}(Re_x) - 0.65]^{2.3} \quad (20)$$

According to T. Maître et al. [9], the laminar, transition and turbulence layers are contained in the following ranges: $y^+ < 5.5 < y^+ < 30.3 < y^+ < 300$ respectively. The linear (laminar) and logarithmic (turbulent) laws-of-the-wall are combined into a single wall law (Wall-law) to assign the velocity to the first cell of the wall grid whatever its value of y^+ .

For the mesh at this point a quadrangular area subdomain is made with its approximate sides to the length of the string see Figure 9. There an O-grid was made with a minimum cell size of $8\mu m$ corresponding to a y^+ of 1, the same y^+ was used on the axis, where the first cell was $5\mu m$.

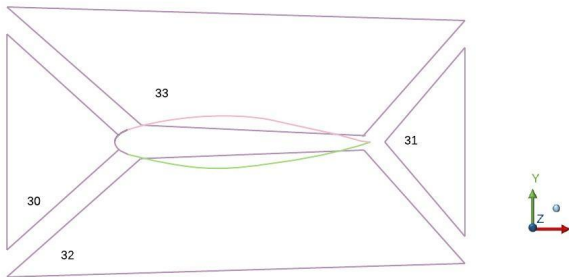


Fig 9. Subdomain detail

2.2.3 Domain

To carry out the simulation it was necessary to use a static domain, where the interference of this in the final result and the convergence time was evaluated, that is why a circular domain recommended by Mäläl [10] and Confluence Cornell [11] was implemented. Having a static round, concentric domain to the rotating domain facilitates mesh generation, as shown in Figure 10.

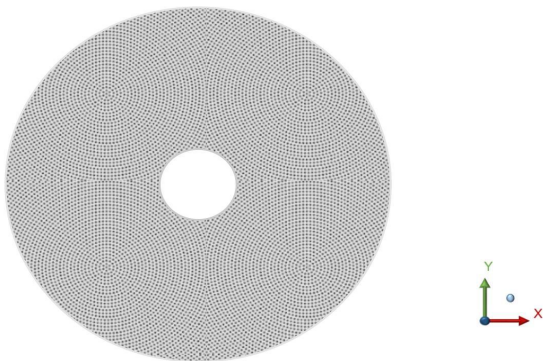


Fig 10. Stator domain

The following three simulations were performed with the transient configurations corresponding to the first TSR: 1 as shown in Figure 11.

It was first tested with 5 times the diameter, then 10 times and finally 20 times the diameter as shown in Fig. 12. The graph shows the results obtained in the 3 cases, in which for the first 5D domain the behavior is periodic after 30 seconds,

the 10D obtained a periodicity after 32 seconds and the 20D had a periodic behavior from 10 seconds.

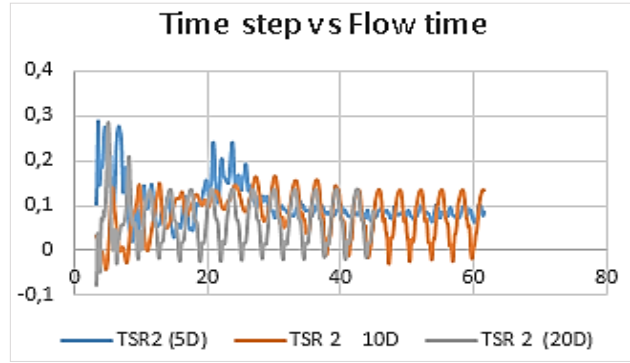


Fig 11. Domain selection DU06-2000W

The first case of 5D is discarded because it presents great differences when compared to the other two; there is a phenomenon known as the boundary effect, in which the contour interferes with the precision of the simulation. In the other two cases the 10D and 20D both reach the same values when they reach the periodic condition, however, it was preferred to choose the mesh with 20D because it reaches these values quickly. The mesh generated with which it is going to work is 1'683.429 nodes.

3. Results

When the solver has stabilized, periodic data are presented which indicate that the simulation has converged. Taking this into account, the following C_m results are obtained for each simulated TSR as shown in Figure 12, corresponding to the last turn of the turbine. To validate the DMST, a Fluent CFD simulation was chosen, evaluating the TSRs point to point, Figure 13.

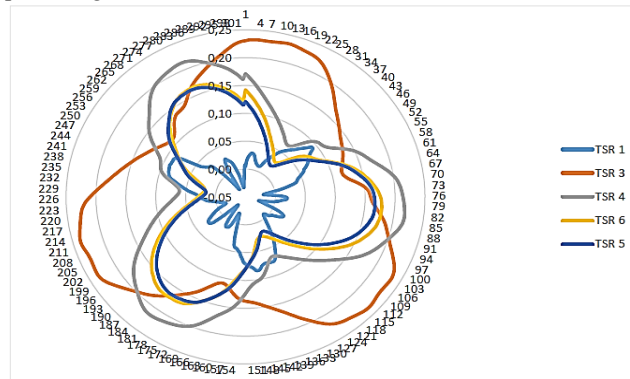


Fig 12. Torque coefficient vs. azimuthal angle

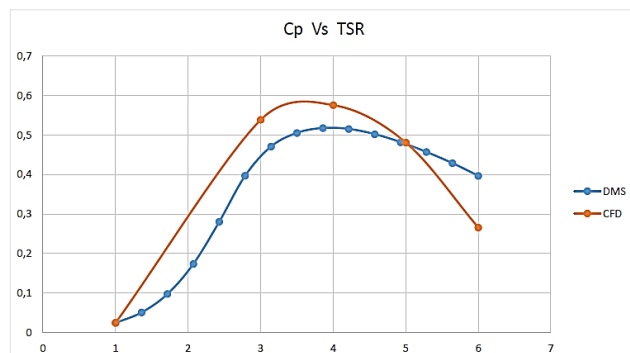


Fig 13. Results for DU06-W200 profile

Both series of data have a good correlation, the CFD line is above the DMST line because in low TSR values the DMST code fails to describe the dynamic loss which generates counterflow and different velocity and pressure gradients in the boundary layer. In high TSR values the code overestimates the CP because it does not take into account side effects such as those generated by the presence of the axis that causes the fluid to lose energy when it collides with it, 4 points were simulated that marked the sufficient tendency to validate the curve.

This behavior is similar to the hydrokinetic turbine simulations performed by S. Lain [12] and Y. M. Dai [13] where the CFD curve was above the DMST.

4. Conclusion

The DU 06-W-200 profile with a C_p of 0.5153 in a TSR 4.2142 is the one that can generate the best output power by taking advantage of 51% of the energy provided by the water, it also has a smoother operation when the TSR values

increase, however in low TSR values the turbine has C_p values close to zero which could lead to auto-start problems. On the other hand, the C_p depends directly on the range of TSRs in which it performs. As the TSR increases the range of angles of attack approaches 0° , generating less lift on the profiles and therefore less power.

As a practice of the Fluent environment, it is observed that to elaborate the Darrieus turbine simulation it is necessary to have a domain of at least 20 D to avoid the boundary effect that affects the accuracy of the results.

5. Acknowledgments

The authors acknowledge the contributions of the company ESSS-Chile to the original version of this document regarding the development of the simulation and the performance of the software.

This is an Open Access article distributed under the terms of the Creative Commons Attribution License



References

- [1] J. Laverde, M. Alzate, F. Aldana, y N. Duarte. Cartilla de servicios públicos para las entidades territoriales. Primera edición. Bogotá, Colombia. 2012.
- [2] H. Sutherland, D. Berg y T. Ashwill, *A retrospective of VAWT Technology*. Inform technical, Sandia National Laboratories, Albuquerque, U.S.A. 2012.
- [3] S. Eriksson, H. Bernhoff y M. Leijon, "Evaluation of different turbine concepts for wind power", *Renewable and Sustainable Energy Reviews*, vol. 12, no.5, pp. 1419-1434, 2008.
- [4] V. Santibáñez, "Estudio experimental de las características de una turbina Darrieus para la marea, generación de energía", *Universidad de Nihon. 132(3)*, pp. 39-45, 2000.
- [5] I. Paraschivoiu. *Wind Turbine Design with Emphasis on Darrieus Concept*. 4th ed. Quebec, Canada. pp. 158-170. 2002.
- [6] A. Mulugeta, A. Somonovic, D. Komarov y S. Stupar, "Numerical and analytical investigation of vertical axis wind turbine", *FME Transactions*, Vol. 4, n° 1, pp. 49-58, 2013.
- [7] B. Montgomerie, "Methods for root effects, tip effects and extending the angle of attack range to $\pm 180^\circ$ to $\pm 180^\circ$, with applications to aerodynamics for blades on wind turbines and propellers", *Swedish Defense Research Agency*. Suecia. pp. 10-54. 2004.
- [8] Ansys Inc. "Ansys Best Practices Manual", *Ansys User Guide*, vol. 1, 2018.
- [9] T. Maitre, E. Amet y C. Pellone, *Modeling of the flow in a Darrieus water: Wall grid refinement analysis*, 1st ed., Paris, Francia. pp. 6-10, 2012.
- [10] I. Mäläel. *Numerical simulation of vawt flow using Fluent*. U.P.B. Sci. Bull. N° 76(1), pp. 109-122 [Online]. Available: https://www.scientificbulletin.upb.ro/rev_docs_arhiva/full6ba_4782_20.pdf
- [11] Cornell University, *FLUENT Learning Modules - SimCafe - Dashboard*, [Online]. Available: <https://confluence.cornell.edu/display/SIMULATION/FLUENT+Learning+Modules>
- [12] S. Lain y C. Osorio, "Simulation and evaluation of straight - bladed Darrieus - type cross flow marine turbine", *Journal of scientific & industrial research*, vol. 69, pp. 906-912, 2010.
- [13] Y. Dai, N. Gardiner, R. Sutton y P. Dyson, "Hydrodynamic analysis models for the design of Darrieus-type vertical-axis marine current turbines". *Proceedings of the Institution of Mechanical Engineers, Part M: Journal of Engineering for the Maritime Environment*, vol. 3, n° 225, pp. 295-307. <http://dx.doi.org/10.1177/1475090211400684>.